Active Vibration Control of Breakup Modes in Loudspeaker Diaphragms

William Cardenas,

KLIPPEL GmbH, Mendelssohnallee 30, Dresden 01309, Germany

One of the factors which contribute to the degradation of the sound quality of the loudspeakers are the breakup modes of the membrane since they cause complex directivity patterns, peaks and deeps in the frequency response. This paper presents an active vibration control simulation applied to a 2D Finite Element model of a loudspeaker loaded by a fluid domain to demonstrate an innovative alternative to reduce the amplitude of the breakup modes of loudspeaker diaphragms, improving substantially the mechanical and acoustical performance. The benefits of the controlled system are demonstrated in terms of the acceleration response of the cone and the acoustic directivity.

1 Introduction

One of the most critical problems associated with the degradation of the sound quality of direct radiation loudspeakers are the breakup modes of the membrane. High acceleration levels of the membrane, corresponding to the low damped resonances, are the causes of the peaks in the sound pressure response. These resonances also present inconvenient directivity characteristics and can contribute to the nonlinearities if the local displacement is large enough [1]. The first frequency which presents a non-rigid body motion behavior is called the break-up frequency and it depends on the mechanical parameters of the material and the geometrical stiffness of the cone [2]. This frequency normally determines the upper limit of the useful band-pass of the loudspeaker and its effect is reduced by using high order crossover networks [3].

Loudspeaker cone vibration has been studied by Kagua [2] using a Finite Element (FE) formulation of a conical shell immersed in a light fluid. In this work, the full coupled system is solved in the axisymmetric coordinate system in the frequency domain. In [12], the vibration of the cone is computed numerically through a FE approach and after the acoustic field is computed by using the velocity profile of the surface. This approximation is valid for cases when the density of the structure is large compared with the fluid density [13], in electroacoustic devices coupled to strong acoustic loads like, vented enclosures or compression chambers the effect of the acoustics on the vibration response is neglected. Other authors such Frankort [14] and Struck [15] have used same numerical schemes to solve the motion equation of the membrane and to perform modal analysis which is the basis of the analysis of the acoustic radiation. One of the interesting application of this methods have been realized by Geaves in [16] who uses the FE and BE methods to select the optimized diaphragm profiles of midrange loudspeakers based on its directivity properties.

Many efforts to reduce the amplitude of the breakup in the Sound Pressure Level response or to shift these phenomena to the high frequencies in order to extend the loudspeaker bandwidth, have been focused on passive techniques. One of them proposes the distribution of the internal damping along the cone surface based in the displacement distribution of the transversal modes [17]. Usually this information is obtained by means of a laser scanner [2] and [10]. Another solution is to attach light sttiffers to the rear part of the membrane to increase the overall rigidity of the system.

In this work, the author studies the possibility to control the modal behavior of the membrane by using an Active Vibration Control (AVC) system similar to those used to control the motion of beams [18], plates [19] and other structures [20] but taking into account that the controller must reduce only the vibrations associated with the non-rigid body motion. For this reason, some modifications have been applied to the Feed-forward structures presented in this references. Many considerations concerning the practical implementation must be taken into account, such as; the efficiency reduction of the loudspeaker due to the incremental mass of the sensors and the cost benefit ratio, considering that each unit should contain a DSP or MCU and a set of transducers among others. This topics will be treated in detail in further publications. In order to show that some important improvements can be achieved in terms of frequency response and sound directivity, numerical simulations concerning the controller performance will be presented. The experimental study will be presented in future works.

The present paper is structured as follows: In the first part, the FE formulation for the fluid-structure interaction is briefly described. In the second part, the specific geometry mesh and the Feed-Forward structure used to control the membrane breakup modes are shown. In the third part, the results of the

simulations are presented along with the deformed mesh of the loudspeaker, the pressure field in the fluid domain and the directivity plots. The paper finishes the discussion of the practical issues and some final remarks.

2 Theoretical description

This section is intended to provide the user a short summary of the background in which this numerical experiment is done, a detailed description on the developments can be found on the cited references.

2.1 FEM Fluid structure interaction

Since this problem involves complex geometries and the motion of the loudspeaker cone cannot be described by analytical functions, a Finite Element formulation for the fluid-structure coupling described in [4], [5] and [6] is adopted. These schemes have been implemented in Matlab®, based on the CALFEM routines.

2.1.1 Acoustic Domain

The nonhomogeneous wave equation for the acoustic pressure in the domain Ω_f can be written as:

$$\frac{\partial^2 p}{\partial t^2} - c_0^2 \nabla^2 p = c_0^2 \frac{\partial q_f}{\partial t} \tag{1}$$

Where $\nabla^2=\partial^2/\partial x^2 + \partial^2/\partial y^2$ is the 2D Laplace operator, p is the acoustic pressure, q_f is the added fluid mass per unit volume and c_0 the propagation sound velocity in the air. After spatial discretization, equation (1) can be written in a matrix form as

$$\mathbf{M}_f \ddot{\mathbf{p}} + \mathbf{K}_f \mathbf{p} = \mathbf{f}_q + \mathbf{f}_s \tag{2}$$

Where the following elementary matrices are defined:

$$\begin{aligned}
\mathbf{M}_f &= \int_{\Omega_f} \mathbf{N}_f^T \mathbf{N}_f \, dS \\
\mathbf{K}_f &= c_0^2 \int_{\Omega_f} (\nabla \mathbf{N}_f)^T \nabla \mathbf{N}_f \, dS \\
\mathbf{f}_s &= c_0^2 \int_{\partial\Omega_f} \mathbf{N}_f^T \nabla p \mathbf{n}_f \, dr \\
\mathbf{f}_q &= c_0^2 \int_{\partial\Omega_f} \mathbf{N}_f^T \frac{\partial q_f}{\partial t} \, dS
\end{aligned} \tag{3}$$

Where $\mathbf{N}_f$ denotes the interpolation function of the fluid domain and $\mathbf{n}_f$ the normal vector to each element on the boundaries. Note that at the fluid-structure interface $\partial\Omega_f$, the interaction of the fluid over the structure will be reported in the term $\mathbf{f}_s$ of (3) [4] and [5].

2.1.2 Structural Domain

In this application, the loudspeaker profile is simplified as a bidimensional array of elastic Bernoully beams [8] and [9]. In a local coordinate system, the frames are governed by the partial differential equation including only the acoustical load.

$$\frac{\partial^2}{\partial x^2}\left(EI \frac{\partial^2 u_s}{\partial x^2} \right) + m \frac{\partial^2 u_s}{\partial t^2} = p(\mathbf{r}, t)\big|_{\partial\Omega_f} \tag{4}$$

Where u_s is the transverse displacement, m is the mass per unit length, EI is the flexural rigidity and p is the acoustic pressure loading the beam in the solid-structure interface $\partial\Omega_f$.

Note that the beam equation element excited by the voice coil force, will include the excitation term corresponding to the axial excitation.

Applying a spatial discretization and using the interpolation functions $\mathbf{N_s}$ [4], [8] and [9] the structural motion equation can be written as

$$\mathbf{M}_s \ddot{\mathbf{d}} + \mathbf{C}\dot{\mathbf{d}} + \mathbf{K}_s \mathbf{d} = \mathbf{f}_f + \mathbf{f}_b \tag{5}$$

Where the elementary matrices in the local coordinate system are written as

$$\begin{aligned}
\mathbf{M}_s &= \int_0^L m \mathbf{N}_s^T \mathbf{N}_s \, dx \\
\mathbf{K}_s &= \int_0^L EI \mathbf{B}_s^T \mathbf{B}_s \, dx \\
\mathbf{C}_s &= \alpha \mathbf{M}_s + \beta \mathbf{K}_s \\
\mathbf{f}_f &= \int_0^L \mathbf{N}_s^T p \, dx \\
\mathbf{f}_b &= \left[\frac{d\mathbf{N}_s}{dx} M - \mathbf{N}_s^T V \right]_0^L
\end{aligned} \tag{6}$$

Note that $\mathbf{B}_s=d^2\mathbf{N}_s/dx^2$ is restricted to one element [4] and [5]. In this case the damping matrix $\mathbf{C}_s$ is computed by means of the damping coefficients α and β in the Rayleigh model [6]. The $\mathbf{f}_f$ term accounts for the effect caused by the fluid over the structure.

2.1.3 Fluid structure Interaction

In the two previous formalisms, the dynamic coupling terms $\mathbf{f}_s$ and $\mathbf{f}_f$ for the structure and fluid domains respectively, need to be reformulated using the shape functions used in each domain [6]. In this coupling, the first boundary condition establishes the continuity of the fluid and the structural displacements in the normal direction of the interface. The matrix H is introduced as a coupling term

$$\mathbf{H} = \int_0^L \mathbf{N}_s^T \mathbf{N}_f \, dx \tag{7}$$

Then, equations (2) and (5) can be rewritten in matrix form as

$$\begin{bmatrix} \mathbf{M}_s & \mathbf{0} \\ \rho c_0^2 \mathbf{H}^T & \mathbf{M}_f \end{bmatrix} \begin{bmatrix} \ddot{\mathbf{d}} \\ \ddot{\mathbf{p}} \end{bmatrix} + \begin{bmatrix} \mathbf{C}_s & \mathbf{0} \\ \mathbf{0} & \mathbf{0} \end{bmatrix} \begin{bmatrix} \dot{\mathbf{d}} \\ \dot{\mathbf{p}} \end{bmatrix} + \begin{bmatrix} \mathbf{K}_s & -\mathbf{H} \\ \mathbf{0} & \mathbf{K}_f \end{bmatrix} \begin{bmatrix} \mathbf{d} \\ \mathbf{p} \end{bmatrix} = \begin{bmatrix} \mathbf{f}_b \\ \mathbf{f}_q \end{bmatrix} \tag{8}$$

This coupled system of equations is reduced by applying the fixed constrain boundary conditions of the structure on the surround and spider ends and

limiting the displacements on the y axis to transversal displacements only. The system with the adaptive controller (introduced in the next section) is finally solved by means of a Newmark algorithm [24].

3 Active Vibration Control Simulation

3.1 Geometry and Mesh

The geometry of the 2D discretization of the fluid domain and the structure geometry are shown in Fig 1.

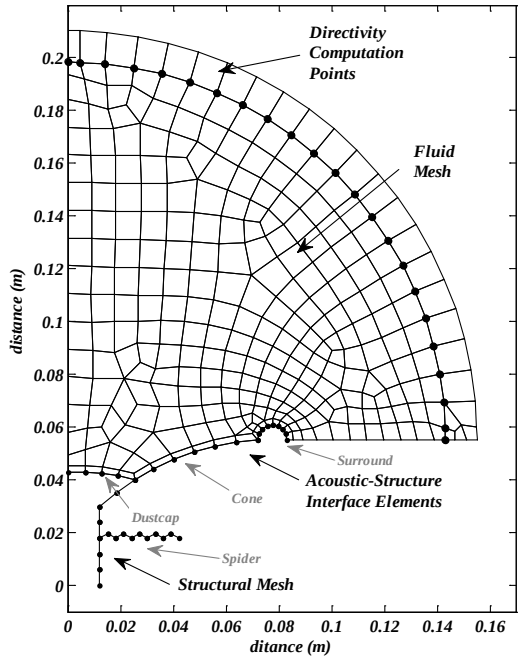

Fig 1. Finite Element Mesh

There are a 35 structural beam type element, with two translation and one rotation degrees of freedom per node for the loudspeaker and 278 linear isoparametric elements for total of 213 Elements and 423 degrees of freedom for the acoustic domain. In this case only the right part of the loudspeaker and the semicircular region of the fluid are meshed. The fluid-structure interface is composed by 18 elements, for which the coupling matrix **H** is computed.
Some pressure nodes located at 0.15 m from the loudspeaker are used to compute the directivity in the near field of the high frequencies. In the global assembling matrix process, the different materials for the elements belonging to the cone, the spider, the dust cap and the surround are defined.

The considered loudspeaker is a 6 in. midrange with curved profile, a curved profile was chosen since it provides a better distribution of the axial load imposed by the voice coil along the cone structure shifting the first breakup mode to the high frequencies. This topology is commonly found in commercial products.

3.2 Control Scheme

The active vibration control has been applied to many different problems including control of plates, beams and conical shells among others [25]. In these applications, the controller is intended to reduce the amplitude of the resonances including the first mode. In the case of the loudspeaker, the first mode cannot be modified by the system because this transfers all the low frequency information of the signal. For this reason it is necessary to modify the existing techniques in order to impose a restriction in the bandwidth of the controller.

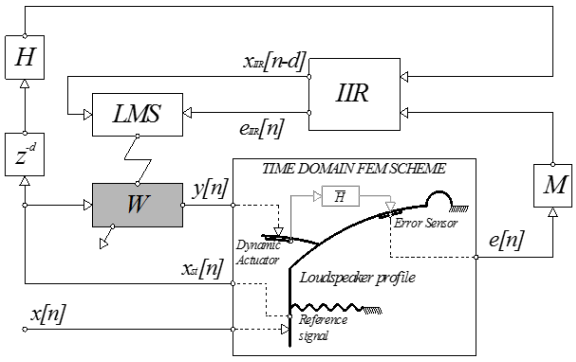

Fig 2. Block diagram of the FX-LMS algorithm

The proposed control technique, used in the AVC application is the FX-LMS structure because of its implementation simplicity and stability [18]. In Fig 2. The block diagram of the FX-LMS used in the simulations is shown. This corresponds to a feed forward controller which reference signal x_{st} comes from the signal applied to voice coil. Note that in the simulation, the electric signal measured in the loudspeaker coil also contains the mechanical reaction of the loudspeaker due to the electromechanical coupling existing in the voice coil. In the model, this is taken into account by using $x_{st}[n]$ as the reference signal rather than $x[n]$, which does not present any mechanical reaction. The filter W is the Finite Impulse Response adaptive filter which is updated each time by using the LMS algorithm as

$$W[n] = W[n-1] - 2\mu e_{IIR}[n] x_{IIR}[n-d] \qquad (9)$$

where μ is the step parameter of the LMS algorithm. This parameter determines the velocity of convergence and the accuracy of the inverse filter [26]. Since the controlled vibration is a linear and time invariant mechanism, the adaptive process is required only for the identification of the signal paths. Note that the signal $x[n]$ takes a time proportional to d samples before arriving to the $e[n]$

position due to the finite propagation velocity of the vibration in the cone material. Note also that the signal $e_{IIR}[n]$ comes from the filtering of $e[n]$ with the sensor transfer function M and the IIR filter $e_{IIR}[n]=(e[n]*M)*IIR$. In the same manner, the signal $x_{IIR}[n]$ must pass through the estimated secondary path H and IIR. In order to have the same sample of the error and the reference signal coming into the LMS algorithm (9), the reference signal should be delayed by a d samples. The adaptive filter output $y[n]$, also called anti-vibratory signal is assigned to the dynamic actuator located in the dust cap.

The secondary path $\hat{H}$ is the transfer function from the output sensor and the error sensor position. In this simulation, this is estimated by computing the impulse response between these two nodes in the FE model.

It is important to remark that the adaptation process will detect only components of the signal allowed in the band pass of the filter. If this band is located around the breakup frequencies of the membrane, the control system will reduce only those components without affecting the rigid body motion of the loudspeaker, see Fig 7.

3.3 Optimal position of sensors based on cone Modal Analysis

The control system reduces effectively the amplitude of the modes which present high displacements in the sensors positions. In order to ensure an appropriate performance of the AVC system, the error sensor should provide enough information about the mode to be attenuated and the dynamic actuator should be far from the nodal lines in order to exert a strong influence in the vibration field of the mode.

To find the optimal positions (node points in the structural mesh) of the error sensor and the dynamic actuator, a modal analysis has been performed, which allows to determine the eigenshapes of the most important resonances in the loudspeaker. In figure 3, the revolution representation of the 2D displacement field for the first mode (rigid body motion) at 80 Hz, the first breakup mode at 1k Hz and one high frequency mode at 6k Hz are depicted.

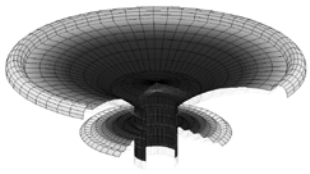

a)

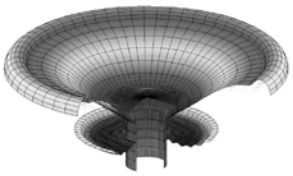

b)

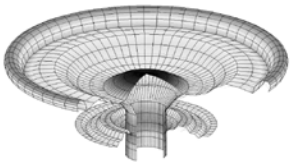

c)

Fig 3. Structural mode shapes of the loudspeaker, a) 80 Hz, b) 1k Hz and c) 6k Hz

The rigid body motion is shown to illustrate the difference with the breakups. Note that the first and the second high frequency modes present a maximum displacement in the center of the dustcup and in the element which connects the cone with the surround. This can be explained, since the surround material has a less stiffness providing an almost free boundary condition to the cone. From this analysis can be concluded that the optimal position for the sensors are those described before. The exciter is placed on the dustcup and the error sensor on the outer part of the cone. To provide a more realistic simulation scenario, the elements in contact with this 2 nodes have eight times the density of the cone material in order to account for the incremental mass of the sensors.

4 Performance of control system

In this section the results of the simulation, comparing the cases with the Active Vibration Control (AVC) in on (active) and off states (inactive), are presented.

4.1 Solution and data extraction

The vibroacoustic system of equations (8) and the controller described in section 3.2 is solved in the time domain in two stages. The first uses a white noise with persistent excitation to allow the adaptive filter IIR to converge and to estimate the secondary path of the transfer function $\hat{H}$. In the second stage the filter coefficients are stored and the adaptive step μ is set to zero and the system is excited by a Delta Dirac signal. The acoustical and structural impulse responses are collected and later transformed into the frequency domain to produce the following results.

4.2 Frequency response

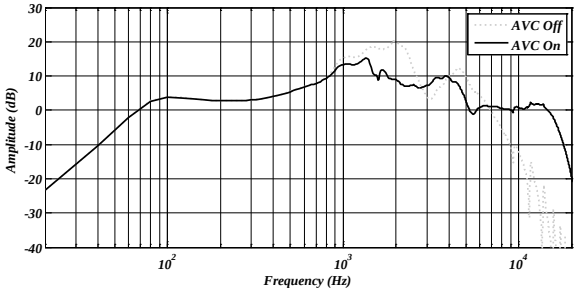

Fig 4. Acceleration response at the error sensor position

In Fig 4 the Frequency Response Functions (FRF) between the acceleration response at the error sensor position and the applied force to the node located at the voice coil are plotted. As expected, the low frequency behaviour of the speaker remains the same and two clear effects can be seen in this figure, the first is the attenuation of more than 10 dB achieved by the controller around 2khz where the modal density is high and the second is the increment of the high frequency components up to 10kHz. The controller imposes a flat and smooth acceleration response reducing the undesired peaks around the breakup region. The acoustic output of this acceleration profile is described in the next section.

4.3 Sound directivity

One of the main motivations in applying the active vibration control to a loudspeaker diaphragm apart from reducing the high level peaks in the SPL response is also to control the directivity of the breakup modes, which presents complex patterns due to its variable velocity profiles [2]. In Fig 5 one time instant of the simulation for the loudspeaker driven by different input sinusoidal signals at 80 Hz, 4.5k Hz and 7k Hz are shown.

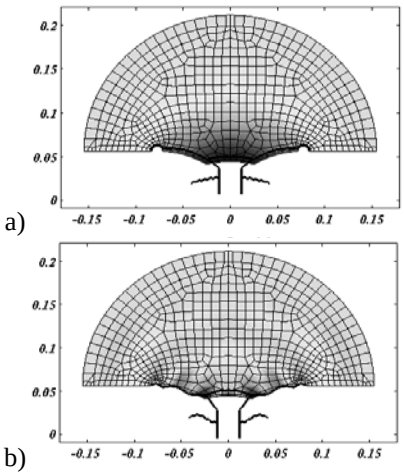

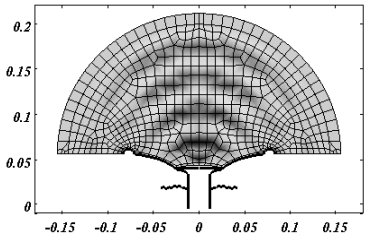

Fig 5. A time instant of the fluid-structure coupling for a different input signals: a) 80 Hz, b) 4.5kHz and c) 7kHz

In Fig 5 the complexity of the near acoustic field produced by the curved radiator is shown. Air compressions and rarefactions are coincident with the deformed structural mesh. In order to compute the near field directivity plots, two layers of proportional damping are introduced in the circular boundary to reduce the level of the reflected wave.

In Fig 6 the impact of the AVC system in the directivity response of the loudspeaker is clearly shown. Since the controlled membrane is more similar to a rigid piston at high frequencies, it is expected that the lateral lobes generated by the breakup deformation of the membrane, become reduced and the principal lobe wider. Note that the acoustic field radiated at 7 kHz comes mainly from the dust cap which dominates the effective radiation surface.

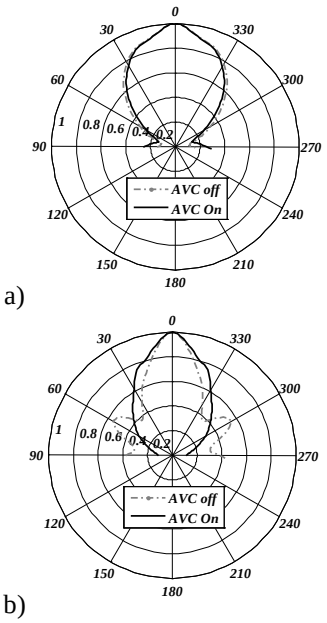

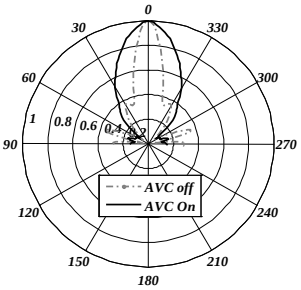

c)

Fig 6. Near field directivity patterns at frequencies in the controlled region, a) 2kHz, b) 4.9kHz and c) 7kHz.

When the controller is active, the lateral lobes are highly attenuated because they are part of the interaction between the dust cap and the rest of the cone. This behaviour brings remarkable benefits for loudspeakers dealing with wideband reproduction because the one lobe behaviour of the controlled directivity produces les interaction with the room producing a better sound image.

On the three plots, the impact of the mesh size on the applied damping which produces more attenuation at the center of the domain due to the accumulation of smaller elements, can be seen, but this approach is valid for the rest of the circumference where the element sizes are equally distributed and the comparison is done in relative terms.

4.4 Optimized Adaptive filter

To create a destructive interference at the error sensor position, the adaptive filter must generate at the actuator position, a signal which contains the same magnitude information but with an inverted phase after being propagated from this position to the error sensor. It means after passed through the secondary path $\hat{H}$ (see Fig 2). In Fig 7, can be seen how after convergence the adaptive filter tries to emulate the magnitude shape of the con vibration, but inverting the phase, in the region delimited by the cutoff frequencies of the IIR filter.

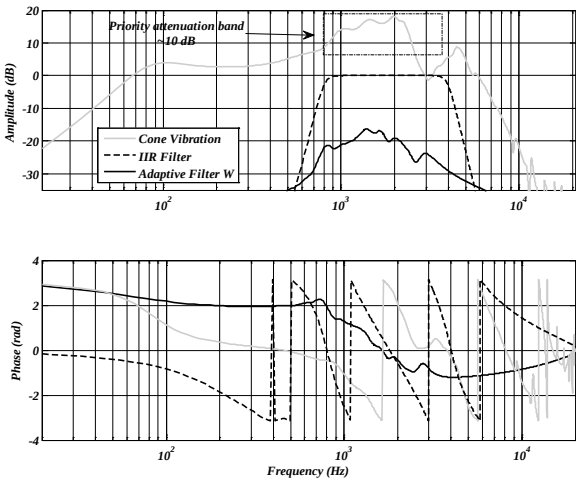

Fig 7. Adjusting the priority band of the controller by setting up the cutoff frequencies of the IIR filter

Note that the convergence must be stopped when the vibration of the cone has been attenuated around 10 dB in these frequencies, otherwise, the filter will introduce a gap, degrading the sound quality of the loudspeaker.

4.5 Practical application and the future of AVC on loudspeakers

The idea of placing two small transducers on the surface of a larger transducer to improve the acoustical performance sounds bit unrealistic and a potential source of new problems as; wideband efficiency reduction due to the added mass of the transducers, the tuning of the system, energy aspects concerning the power of the DSP and required electronics. Nevertheless there are many applications like small studio monitors, hi-fi systems where one driver needs to reproduce wide range of frequencies, where an attenuation of 10 dB of the modal resonances and smooth directivity will increase considerably the sound quality of such a products.

Considering the processing power and prices of new microcontrollers and microprocessors, nowadays is possible to include digital signal processing closed to the transducer to correct electronically the physical weakness of the electromechanical system. Since the breakup modes are a distributed parameter problem governed by partial differential equations, a distributed control technique is required. This paper was written to proof the concept that an Active Vibration Control on cones can dramatically improve some of the most important deficiencies of loudspeakers related with each structural nature,it is hoped that this can be implemented based on new

material technologies and smart adaptive structures in an near future. Before this time is reached, this paper is considered a purely academic work

5 Conclusions

This paper corroborates that an active vibration control of the breakup modes is, at least in theory, possible and brings very important improvements of the loudspeaker performance in terms of the frequency response and acoustic directivity. It has been demonstrated that is possible to achieve more than 10 dB attenuation of the peaks caused by cone breakups in the band pass of the adaptive filtering as well as to reduce the presence of secondary lobes in the same region. This increases dramatically the performance of some loudspeaker drivers required to operate on the full frequency range.

The simulation of an Active Vibration Control system, based on a modified FX-LMS algorithm, is presented by using a 2D fluid-structure interaction model of a loudspeaker. This model has been solved in the time domain by integrating the vibroacoustic FEM equations using the Newmark-β algorithm.

A modification of the conventional FX-LMS algorithm for feed-forward structures has been proposed, by including a high order filter in the reference and error signals, in order to limit the bandwidth of the controller. This modification allows not only attenuating only the excess of vibration at the breakup region but also leaving unmodified the rigid body motion of the transducer.

The system minimizes the required amount of resources, in terms on sensors and processing units to control a complex distributed displacement field, optimizing the sensors position using the modal analysis of the loudspeaker structure.

This work is a good example to demonstrate that the combination of some mathematical tools like numerical computation and signal processing allows to think on new solutions to improve the loudspeaker quality using technologies that are not implemented in real life, but can conduct to new alternatives for future materials used in loudspeaker industry.

References

[1] Klippel W. “Tutorial: Loudspeaker nonlinearities – causes, parameters symptoms”. J Audio Eng Soc 2006;54(10):907-39.

[2] Klippel W. J Schclechter, “Distributed Mechanical Parameters of Loudspeakers, Part 2: Diagnostics”. J Audio Eng Soc 2009;57(9):696 – 708.

[3] Davis D. Ptronis E, “Sound System Engineering Third Edition”, Focal press, 2006.

[4] M. Ristinmaa, G. Sandberg, and K-G. Olsson, “Fundamentals of Fluid-Structure Interaction, Department of Construction Sciences, Structural Mechanics, Lund University, Lund.

[5] Maxwell C. “A Simple Simulation of Acoustic Radiation from a Vibrating Object” Presented at the 123rd Convention 2007 October 5-8 New York, NY.

[6] M. Ristinmaa, G. Sandberg, and K-G. Olsson, “CALFEM. A finite element toolbox to MATLAB, Version 3.4, StructuralMechanics and Solid Mechanics, Department of Mechanics and Materials, Lund University, Sweden, 2004.

[7] G.C. Everstine, “Finite element formulatons of structural acoustics problems” Computers & Structures, Volume 65, Issue 3, November 1997, Pages 307–321

[8] O. C. Zienkiewicz and R. L. Taylor, Finite Element Method: Volume 1, The Basis, chapter 19, pp. 542–574, Butterworth-Heinemann, 2000.

[9] Y. W. Kwon and H. Bang, The finite element method using MATLAB, CRC Press, 2000.

[10] Visualization of vibration of loudspeaker Membranes,Schlechter J. Thecnical University of Dresden

[11] Kagawa, Y., Yamabuchi, T., Sugihara, K. and Shindou, T., A finite element approach to a coupled structural-acoustic radiation system with application to loudspeaker characteristic calculation. Journal of Sound and Vibration, 1980, 69(2), 229-243

[12] A. J. M. Kaizer, A. D. Leeuwestein, “ Calculation of the Sound Radiation of a Nonrigid Loudspaker Diaphragm Using the Finite-Element Method,” J. Audio Eng. Soc., Vol. 36, No. 7/8, 1988 July/August, pp. 539 – 551

[13] Fahi F, “Sound and Structural Vibration”. Academic Press, 2007

[14] F.J.M. Frankort, “Vibration Patterns and Radiation Behavior of Loudspeaker Cones,” J. of Audio Eng. Soc., Sept. 1978, Vol. 26, pp. 609- 622

[15] C. Struck, “Analysis of the Nonrigid Behavior of a Loudspeaker Diaphragm using

Modal Analysis," presented at 86th convention of Audio Eng. Soc., Hamburg, 1989, preprint 2779

[16] Geaves, Gary P. "Design and Validation of a System for Selecting Optimized Midrange Loudspeaker Diaphragm Profiles". J Audio Eng Society Volume 44 Issue 3 pp. 107-118; March 1996

[17] T. Heed, "Minimizing the Amplitude of Transverse Modal Waves in Diaphragms," presented at the 101st Convention of the Audio Eng. Soc., November 1996, Los Angeles, preprint 4333

[18] Elliott, S. J., 2001. "Signal Processing for Active Control". Academic Press, London

[19] Leniowska, "Effect of active vibration control of a circular plate on sound radiation l". archives of acoustics 31, 1, 77–87 (2006)

[20] Resonant Control of Structural Vibration Using Charge-Driven Piezoelectric Actuators

[21] Loutridis, Resonance identification in loudspeaker driver units: A comparison of techniques. Applied Acoustics

[22] Janse CP, Kaiser A. Time–frequency distributions of loudspeakers, the application of the Wigner distribution. J Audio Eng Soc 1983;31(4):198–209

[23] Wehbner. K, The Finite Elemnt Method for Engineers, John Willey & Sons, 2001

[24] Zampieri E, Pavarino F , "Approximation of acoustic waves by explicit Newmark's schemes and spectral element methods", Journal of Computational and Applied Mathematics, Volume 185, Issue 2, 15 January 2006, Pages 308–325

[25] Feng-Ming Li1," Active vibration control of conical shells using piezoelectric materials " Journal of Vibration and Control, Dic 16 2011

[26] Muhammad T, Mitsuhashi W, " Improving performance of FxLMS algorithm for active noise control of impulsive noise" Journal of Sound and Vibration, Volume 327, Issues 3–5, 13 November 2009, Pages 647–656